Journal of Applied Fluid Mechanics, Vol. 17, No. 8, pp. 1618-1630, 2024.
Available online at www.jafmonline.net, ISSN 1735-3572, EISSN 1735-3645.
https://doi.org/10.47176/jafm.17.8.2445

Numerical Study of the Mixing Process during Hydrogen Blending in Natural Gas Pipelines

J. Du, X. F. Lv, H. J. Zhao†, S. W. Qiao, and Z. H. Chen

Jiangsu Key Laboratory of Oil and Gas Storage and Transportation Technology, Changzhou University, Changzhou, Jiangsu Province, 213100, China
School of Petroleum and Natural Gas Engineering, Changzhou University, Changzhou, Jiangsu Province, 213100, China

†Corresponding Author Email: zhj@cczu.edu.cn

ABSTRACT

An uneven mixing of hydrogen-blended natural gas will lead to hydrogen embrittlement in distribution pipelines, thereby affecting the quality of terminal gas, and thus highlighting the importance of ensuring the uniformity of hydrogen and natural gas mixing. In this study, FLUENT software was used to simulate three different hydrogen filling modes, namely, T-tube, bending-tube, and static mixer, and the mechanisms underlying the mixing of hydrogen and natural gas under different filling modes were analyzed. In addition, we assessed the influences of gas velocity, hydrogen blending ratio, and mixer length and blade angle on the mixing effects of a static mixer. The results revealed that among the three mixing methods assessed, the static mixer has the best overall mixing effect. Increasing gas velocity was found to have no significant effect on the mixing of hydrogen and natural gas. With an increase of hydrogen blending ratio, the mixing uniformity of hydrogen and natural gas increased from 99.49% to 99.95%, whereas there was an increase from 84.12% to 99.05% when the length of static mixer was increased, and an increase from 59.53% to 99.78% in response to an increase in blade angle. Our findings in this study can provide a methodological reference for increasing the mixing uniformity of hydrogen and natural gas in hydrogen-blended natural gas pipeline networks, and thereby contribute to the safe and rapid development of the hydrogen energy industry.

Article History

Received November 22, 2023
Revised January 19, 2024
Accepted February 2, 2024
Available online May 29, 2024

Keywords:

Hydrogen blending ratio
Hydrogen-blended natural gas
Mixing uniformity
Static mixer
Species transport model

1. INTRODUCTION

Hydrogen energy is a globally recognized source of clean energy with the advantages of abundant sources, high combustion calorific value, and harmless combustion products (Mazloomi & Gomes, 2012; Yuxuan, 2022), and is considered the "ultimate energy" of human society. The United States, China, European Union, and other countries and organizations have accordingly issued relevant policies to promote the development of hydrogen energy (SHhangze et al., 2022). At present, mixing hydrogen into natural gas pipelines and using existing natural gas pipelines for transportation are the main methods of utilizing hydrogen energy (Zhen et al., 2021), and although countries such as The Netherlands, France, and Australia have carried out demonstration projects for evaluating the mixing hydrogen with natural gas (Bing et al., 2022), owing to differences in the densities of natural gas and hydrogen, uneven mixing of these two gases may occur, thereby leading to hydrogen accumulation and pipeline embrittlement (Dadfarnia et al., 2019; Yuxin et al., 2022; Wei et al., 2023), ultimately affecting the safety of terminal natural gas (Shijie et al., 2019; Fang et al., 2023).

Among the scholars who have studied the factors influencing the mixing of natural gas and hydrogen, Cuiwei et al. (2022) examined the distribution regularities of the hydrogen volume fraction of hydrogen-blended natural gas under conditions of cylinder storage, pipeline shutdown, and flow. In addition, Hongjun et al. (2022) simulated gas stratification during the static placement of fluctuating hydrogen-blended natural gas pipelines and studied the influence of terrain drop and hydrogen blending ratio. The results revealed that the greater the difference in the fluctuation height of the pipelines, the higher was the volume fraction of hydrogen accumulating in the top of horizontal pipes after reaching a stable stratification. Furthermore, Yongwei et al. (2022) studied the accumulation of hydrogen in T-type and variable-diameter hydrogen-mixing pipelines, and accordingly found that hydrogen readily accumulated in the variable-diameter section, resulting in hydrogen embrittlement.

NOMENCLATURE

β_i	constant	i	type of fluid
Γ_k	effective diffusion coefficient of k	k	turbulent kinetic energy
Γ_ω	effective diffusion coefficient of ω	p	pressure
ρ	fluid density	R_k	constant
σ_k	turbulent Prandtl numbers of k	S_k	user defined source items
σ_ω	turbulent Prandtl numbers of ω	S_ω	user defined source items
D_ω	cross diffusion term	t	turbulent kinetic energy
f_i	unit volume force	u_i	velocity component in each direction
G_b	effect of buoyancy on turbulence	Y_k	turbulence caused by diffusion
G_k	turbulent kinetic energy generated by the laminar velocity gradient	Y_i	volume fraction of each component of the fluid
G_ω	turbulent kinetic energy generated by the ω equation	Y_ω	turbulence caused by diffusion
$G_{\omega b}$	effect of buoyancy on turbulence		

In further studies, Hongjun et al. (2023) examined the mixing of hydrogen injected into hydrogen-blended natural gas pipelines at different sites in high-pressure natural gas pipelines and compared and analyzed the influence of different hydrogen injection amounts and diameters of hydrogen injection pipes on the mixed gas. Similarly, Eames et al. (2022) assessed the effects of the hydrogen injection velocity, hydrogen injection tube diameter, and hydrogen pipeline orientation on the mixing of hydrogen and natural gas in a T-tube.

As efficient mixing equipment, static mixers have been applied in chemical, food, textile, light, and other industries, with good results being obtained, and a number of researchers have applied static mixers for the mixing of hydrogen and natural gas. For example, Yue et al. (2023) investigated the mixing of hydrogen and natural gas in a static mixer, and accordingly found that the mixing uniformity of hydrogen and natural gas increased rapidly after full contact in the mixer. Liu et al. (2022) compared the influence of four static mixers on the gas-mixing process in an F-type pipeline and examined the effects of the main geometric parameters on mixer performance. Liu et al. (2023) also assessed the effects of the number of mixing components, gas velocity, and hydrogen blending ratio on mixing using an SMX static mixer.

However, as previously mentioned, most of the studies on static mixers performed to date have tended to focus on the influence of fluid parameters on the uniformity of mixing, whereas little attention has been paid to the influence of the static mixer geometric parameters on the uniformity of mixing. Consequently, in this study, we sought to compare the influence of three different mixing methods on the uniformity of mixing and analyzed the mixing mechanisms of a static mixer. In addition, we also analyzed the influence of static mixer geometric parameters on the uniformity of mixing. We believe that the findings of this study will make a significant contribution to enhancing the mixing of hydrogen and natural gas, as well as the development of new designs for static mixers.

2. Model and Methods

2.1 Mathematical Model

For the purposes of this study, we used a species transport model to simulate the flow and mixing of natural gas and hydrogen in pipelines, and accordingly confirmed that the flow satisfied the continuity and momentum equations. Given that the SST k- ω model takes into account the propagation of turbulent shear stress, it has higher accuracy and credibility in a wide range of flow fields, and is suitable for simulating the mixing of gases. The specific control equations are as follows.

The continuity equation is as follows:

$$\frac{\partial p}{\partial t}+\frac{\partial(\rho u_i)}{\partial x_i}=0, \tag{1}$$

where ρ is the fluid density, t is time, and u_i is the velocity component in each direction.

The momentum equation is as follows:

$$\frac{\partial(\rho u_i)}{\partial t}+\frac{\partial(\rho u_i u_j)}{\partial x_i}=\frac{\partial p}{\partial i}+\frac{\partial \tau_{xi}}{\partial x}+\frac{\partial \tau_{yi}}{\partial y}+\frac{\partial \tau_{zi}}{\partial z}+\rho f_i \tag{2}$$

where u_i is the velocity component in each direction, p is the pressure, f_i is the unit volume force, and $\tau_{xi}, \tau_{yi}, and\ \tau_{zi}$ are the viscous stress components.

The species transport equation is as follows:

$$\frac{\partial}{\partial t}(\rho Y_i)+\frac{\partial}{\partial x_i}(\rho u_i Y_i)=0, \tag{3}$$

where i is the type of fluid and Y_i is the volume fraction of each fluid component.

The turbulence equations are as follows:

$$\frac{\partial}{\partial t}(\rho k)+\frac{\partial}{\partial x_i}(\rho k u_i)=\frac{\partial}{\partial x_i}(\Gamma_k\frac{\partial k}{\partial X_j})+G_k-Y_k+S_k+G_b \tag{4}$$

$$\frac{\partial}{\partial t}(\rho \omega)+\frac{\partial}{\partial X_i}(\rho \omega u_i)=\frac{\partial}{\partial X_i}(\Gamma_\omega\frac{\partial k}{\partial X_i})+G_\omega-Y_\omega+D_\omega+S_\omega+G_{\omega b} \tag{5}$$

where k is the turbulent kinetic energy; G_k is the turbulent kinetic energy generated by the laminar velocity gradient; G_ω is the turbulent kinetic energy generated by the ω equation; Γ_k and Γ_ω are the effective diffusion coefficient of k and ω; Y_k and Y_ω are the turbulence caused by diffusion; D_ω is a cross diffusion term; S_k and S_ω are user defined source items; and G_b and $G_{\omega b}$ are the effects of buoyancy on turbulence.

$$\Gamma_k = \mu + \frac{\mu_t}{\sigma_k} \tag{6}$$

$$\Gamma_\omega = \mu + \frac{\mu_t}{\sigma_\omega} \tag{7}$$

$$\mu_t = \alpha^* \frac{\rho k}{\omega}, \tag{8}$$

where σ_k and σ_ω are the turbulent Prandtl numbers of k and ω, respectively.

$$\sigma_k = \frac{1}{F_1 / \sigma_{k,1} + (1 - F_1) / \sigma_{k,2}} \tag{9}$$

$$\sigma_\omega = \frac{1}{F_1 / \sigma_{\omega,1} + (1 - F_1) / \sigma_{\omega,2}} \tag{10}$$

$$F_1 = \tanh\left(\Phi_1^4\right) \tag{11}$$

$$\Phi_1 = \min\left[\max\left(\frac{\sqrt{k}}{0.09\omega y}, \frac{500\mu}{\rho y^2 \omega}\right), \frac{4\rho k}{\sigma_{\omega,2} D_\omega^+ y^2}\right] \tag{12}$$

$$D_\omega^+ = \max\left[2\rho \frac{1}{\sigma_{\omega,2}} \frac{1}{\omega} \frac{\partial k}{\partial X_j} \frac{\partial \omega}{\partial X_j}, 10^{-10}\right] \tag{13}$$

The coefficient α^*, which damps the turbulent viscosity causing a low-Reynolds number correction, is determined using the following equation:

$$\alpha^* = \alpha_\infty^* \left(\frac{\alpha_0^* + \mathrm{Re}_t / R_k}{1 + \mathrm{Re}_t / R_k}\right) \tag{14}$$

$$\mathrm{Re}_t = \frac{\rho k}{\mu \omega} \tag{15}$$

$$\alpha_0^* = \frac{\beta_i}{3} \tag{16}$$

where R_k and β_i are defined as two constants, the values of which are 6 and 0.072, respectively.

2.2 Geometric Model and Mesh Division

To mesh the calculation area, we used MESHING software, and to improve mesh quality, mesh encryption was performed near the bending pipe and the static mixer. The geometric model and mesh divisions of T-tube, bending tube, and static mixer mixing are shown in Figs 1, 2, and 3, respectively, and the structure of the static mixer is shown in Fig. 4.

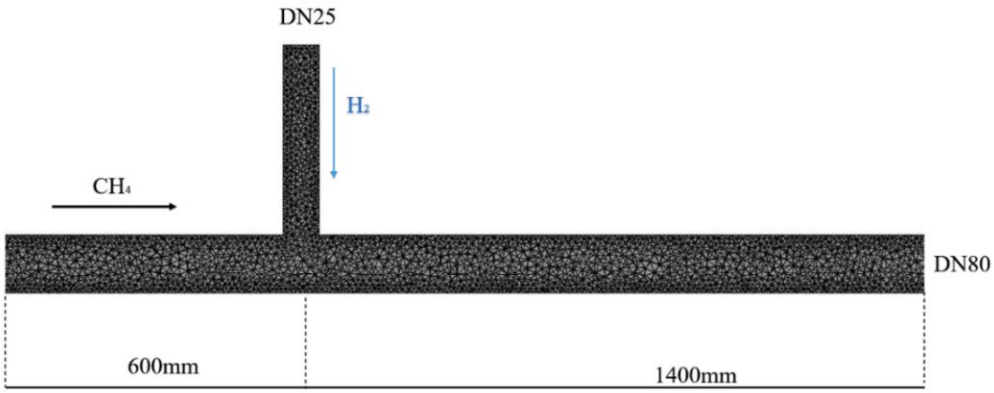

Fig. 1 T-tube mixing

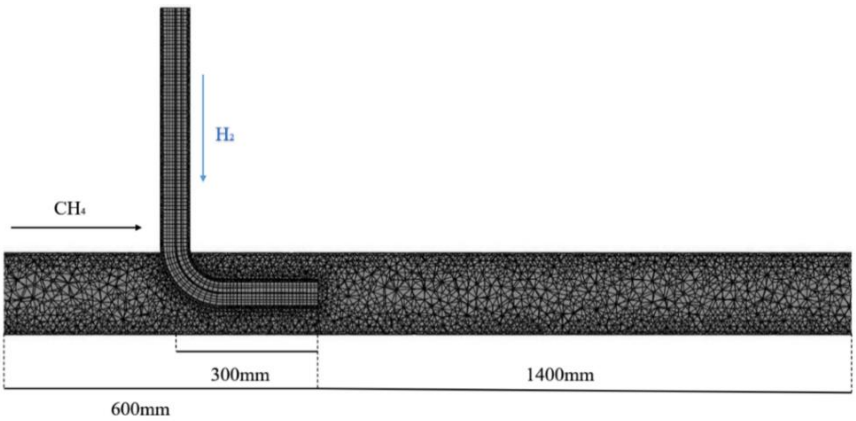

Fig. 2 Bending tube mixing

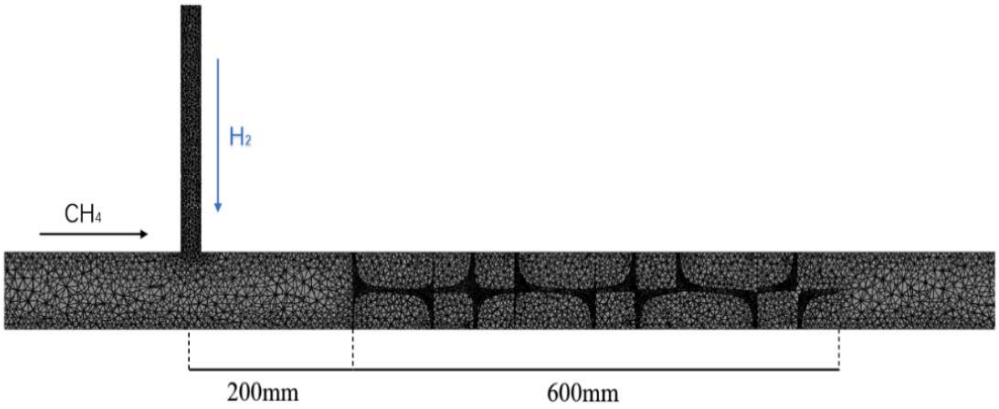

Fig. 3 Static mixer mixing

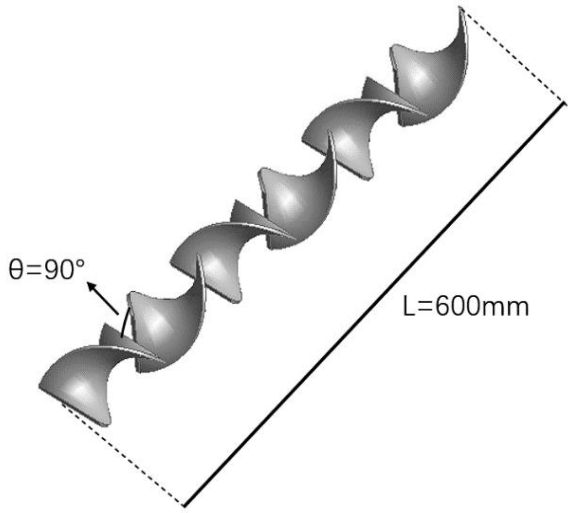

Fig. 4 Structure of the static mixer

2.3 Numerical Method and Boundary Conditions

In this study, we selected a pressure-based solver, and set the reference pressure to a standard atmospheric pressure of 101325 Pa. Gravity was 9.81 m²/s along the Z-axis. The pressure–velocity coupling method was coupled, and the gradient calculation was based on a least-squares cell-based method. The discrete scheme of all equations adopts a first-order upwind. The convergence criterion was set to a residual of less than 10^{-6}. The material data for methane and hydrogen were selected from the FLUENT database.

Boundary conditions: According to the Technical Regulations of the Natural Gas Hydrogen Mixing Station, the pressure before hydrogen and natural gas mixing should be stabilized at a natural gas transmission pressure of +0.05–0.1 MPa, based on reference to the design pressure of the first hydrogen mixing high-pressure gas pipeline in China at 6.3 MPa. For the purposes of the present study, we set the inlet pressures of CH_4 and H_2 to 6.3 and 6.4 MPa; respectively. At the inlet of the natural gas pipeline, the volume fraction of methane is set to 1 and the volume fraction of hydrogen is set to 0, or the volume fraction of hydrogen is set to 1 and the volume fraction of methane is set to 0. Details of the boundary conditions are listed in Table 1.

Table 1 Boundary conditions

	Natural gas inlet	Hydrogen inlet	Outlet	Pipe wall
Type	Velocity inlet	Velocity inlet	Outflow	Wall
Velocity	5 m/s	17.07 m/s	No setup	No setup
Pressure	6.3 MPa	6.4 MPa	No setup	No setup

2.4 Grid Independence Verification

Taking the direction of natural gas flow as the positive direction of the X-axis, we calculated the hydrogen volume fractions at 50, 100, 200, 400, 900, and 1400 mm after the mixing point along the central line of the pipeline using FLUENT when the number of grids (N) was 130,000, 175,000, 310,000, and 600,000. Figure 5 shows the variations in hydrogen volume fraction at the six monitoring points under different grid numbers when the calculation reached a steady state. It can be seen from the figure that a mesh number of 310,000 can better balance the calculation efficiency and accuracy of results, and consequently, we selected this value when performing the numerical simulation calculations.

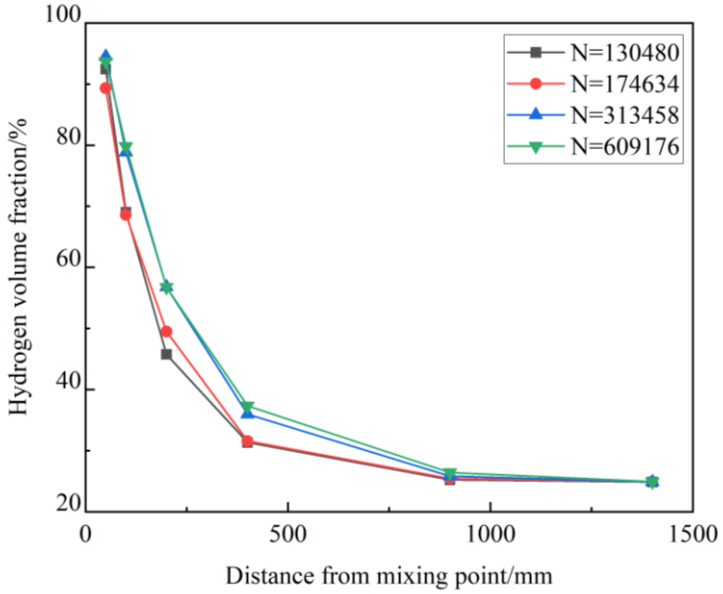

Fig. 5 Variations in the hydrogen volume fraction at different monitoring points under different grid numbers

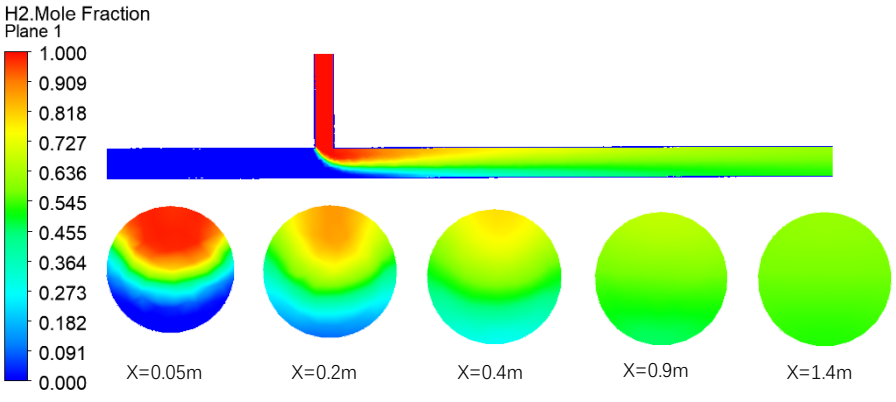

Fig. 6 Contours of the hydrogen mole fraction using T-tube mixing and the contours of cross-sections

2.5 Mixing Uniformity

Mixing uniformity can be characterized by mixing non-uniformity; that is, the root-mean-square deviation of the concentration COV, which is defined as the root-mean-square deviation of the concentration value at the sampling point from the mean value of the concentration at all sampling points, and can be derived using the following equation:

$$COV = \frac{1}{\bar{c}}\sqrt{\frac{\sum_{i=1}^{n}(c_i-\bar{c})^2}{n-1}} \times 100\%, \tag{17}$$

where c_i is the volume fraction of hydrogen gas at a sampling point, $\bar{c}$ is the average volume fraction of hydrogen gas at all sampling points, and n is the number of sampling points.

As implied in its definition, COV represents the degree of difference between the hydrogen volume fraction at each sampling point and the average hydrogen volume fraction of the entire region in the area under investigation. The smaller the degree of concentration difference, the smaller is the concentration gradient and the more evenly the mixture is mixed.

The gas mixing degree σ can be defined as follows:

$$\sigma = 100\% - COV \tag{18}$$

In general engineering, a σ value >95% is considered to be indicative of uniform mixing (Mingxing, 2012).

3. Results and Discussion

3.1 The Effects of Different Filling Methods on the Uniformity of Mixing

To examine the influence of different filling modes on the degree of mixing, we simulated three different mixing modes, namely, T-tube, bending tube, and static mixer mixing. Figure 6 shows the contours of the mole fraction of hydrogen mixed in the T-tube and the contours of the cross-section at X m after the mixing point. As shown in the figure, after hydrogen enters the natural gas pipeline, it initially migrates to the vicinity of the upper pipe wall,

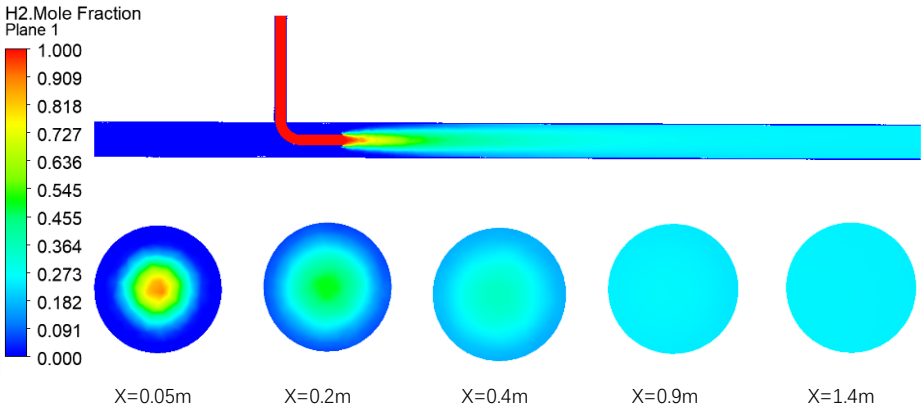

Fig. 7 Contours of the hydrogen mole fraction using bending tube mixing and the contours of cross-sections

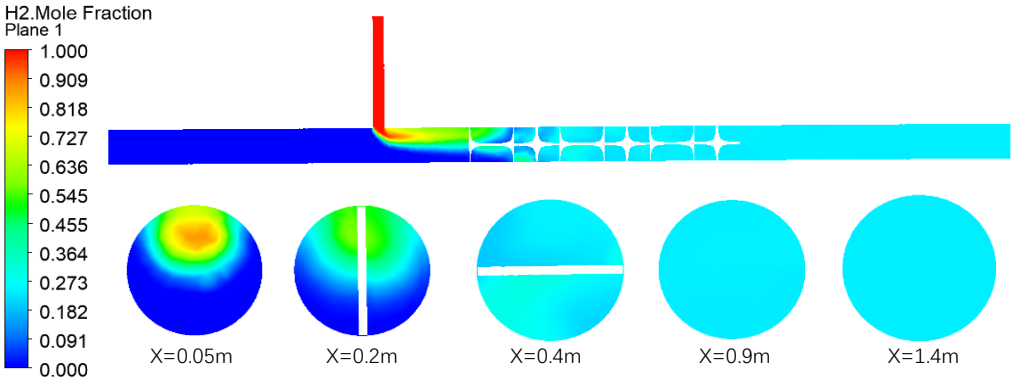

Fig. 8 Contours of the hydrogen mole fraction using static mixer mixing and the contours of cross-sections

and there is a clear concentration gradient in the pipeline, which can be attributed to the fact that the density of hydrogen is less than that of natural gas, and there are differences in the velocity and direction of hydrogen and natural gas flows. The closer the mixing point, the larger is the mole fraction of hydrogen in the middle and upper parts of the pipeline, although there is still an obvious stratification phenomenon at X = 0.4 m. After migrating a sufficiently long distance, the natural gas and hydrogen gradually undergo an even mixing. At X = 0.9 m, the stratification phenomenon has essentially disappeared, and at X = 2.0 m, there is no clear stratification.

The results of mixing natural gas and hydrogen in a bending tube are shown in Fig. 7. After reaching the mixing point, hydrogen is mainly concentrated in the middle of the pipeline and is characterized by a symmetrical tongue-shaped distribution. During hydrogen migration, the volume fraction of hydrogen along the central axis of the pipeline undergoes a rapid decline, whereas the mole fractions of hydrogen along the top and bottom of the pipeline increase rapidly. After the mixing point X = 0.9 m, there was no obvious stratification.

The results of mixing natural gas and hydrogen in the static mixer are shown in Fig. 8. On entering the natural gas pipeline, the hydrogen accumulates in the middle and upper parts of the pipeline, and there is still a clear stratification in front of the static mixer entrance (X = 0.2 m). Mixing tends to be complete at the exit of the first group of static mixers (X = 0.4 m), and there is no obvious

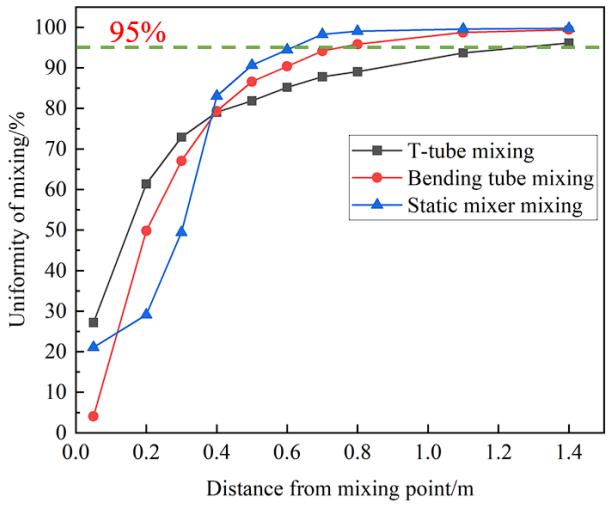

Fig. 9 Variations in the uniformity of mixing using three blending methods

stratification at the exit of the static mixer (X = 0.9 m) or the outlet of the pipeline (X = 1.4 m).

Figure 9 shows the variation in the mixing uniformity of mixing σ with increasing distance from the mixing point using the three different mixing methods, and Fig. 10 presents a streamline diagram depicting mixing using the three different mixing methods. An enlarged view of

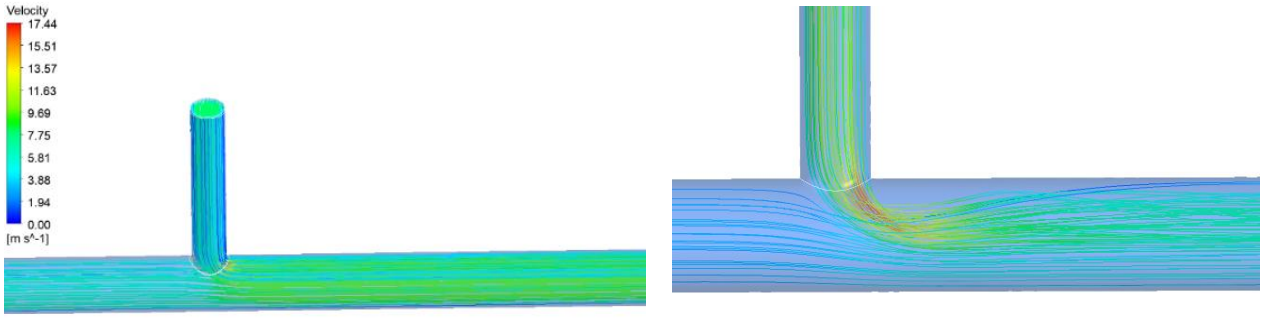

(a) (a)

Fig. 10 An enlarged views of sections of pipeline near the mixing point

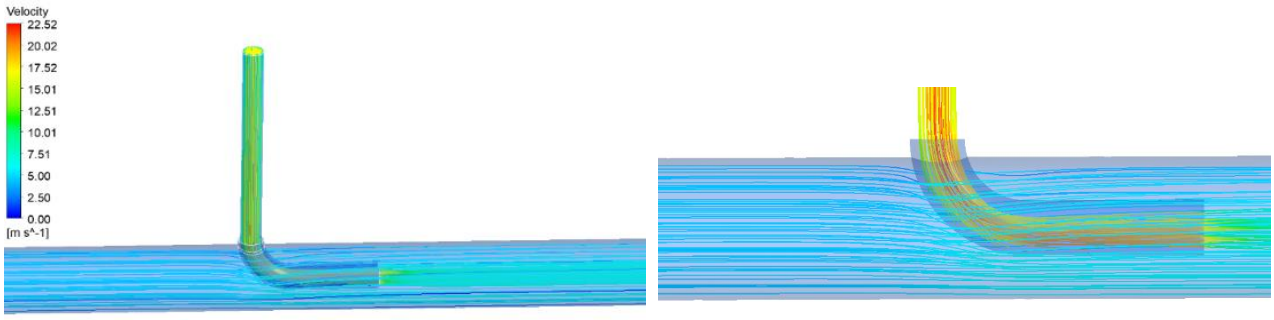

(b) (b)

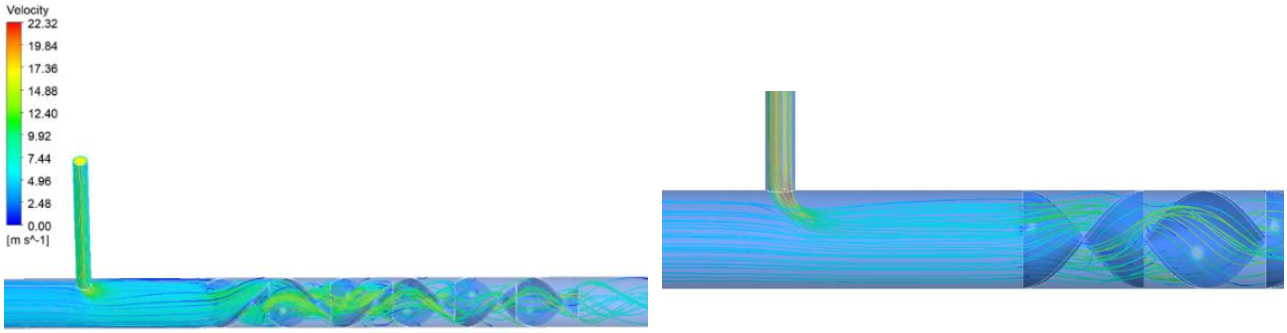

(c) (c)

Fig. 11 A streamline diagram showing the mixing of hydrogen and natural gas using the three mixing methods

the mixing point is shown in Fig. 11.

From Figs 9 and 10, it can be seen that for all three methods, the uniformity of mixing increases with an increase in mixing distance. When using a T-tube for mixing, the hydrogen gas primarily accumulates in the upper part of the pipeline, and as shown in Fig. 11 (a), owing to differences in the initial flow directions of hydrogen and natural gas, there is a high flow velocity in the vicinity of the mixing point, and the intensity of turbulence near the mixing point is also high. However, given that the flow velocity of natural gas is considerably greater than that of hydrogen gas, the direction of the flow of hydrogen undergoes rapid changes, and there is a corresponding reduction the intensity of turbulence. Consequently, a long distance is necessary to achieve uniform mixing, with the mixing uniformity at the pipeline outlet being $\sigma = 96.13\%$. Using a bending tube for mixing, the hydrogen gas enters the middle of the pipeline, as shown in Fig. 11 (b). Given the presence of the hydrogen injection pipe, it is necessary for the upstream natural gas to bypass this pipe, and in doing so, it undergoes shearing with the hydrogen gas. The high intensity of turbulence before and after the hydrogen injection pipe is conducive to the mixing of hydrogen and natural gas. Compared with T-tube mixing, there is a reduction in the distance required to achieve uniform mixing using the bending tube, along with a corresponding reduction in the uniformity of mixing at the pipeline outlet ($\sigma = 99.40\%$). As shown in Fig. 11 (c), there are increases in the flow velocities of hydrogen and natural gas when using a static mixer for mixing, accompanied by a high intensity of turbulence. Moreover, having passed the static mixer, the hydrogen and natural gas continue to flow in a spiral shape, which

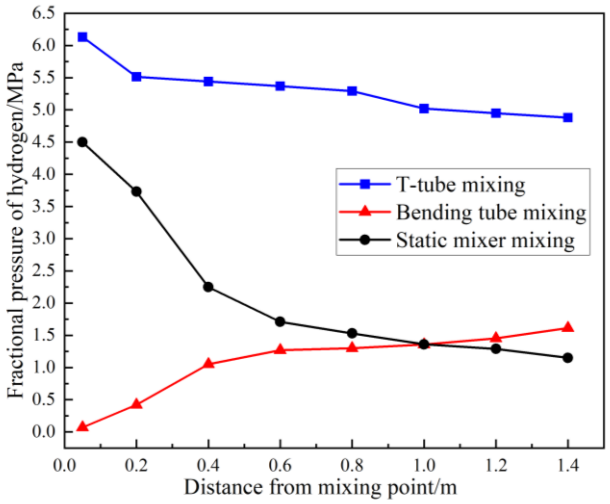

Fig. 12 Variations in hydrogen fractional pressure at different natural gas velocities

is conducive to the mixing of these two gases. Consequently, the distance required to achieve uniform mixing is the shortest among the three assessed systems, and uniform mixing is achieved at the outlet of the pipeline (σ = 99.78%).

As indicated in Fig. 9, there are only marginal differences among the three different mixing methods with respect to the distance required to reach blending uniformity. Accordingly, we subsequently sought to establish the criticality of the mixing length necessary for hydrogen embrittlement.

Previous studies have shown that the total and fractional pressures of hydrogen can influence the sensitivity of materials to hydrogen embrittlement in the presence of hydrogen-blended natural gas. Taking China's X80 steel long-distance natural gas transport pipeline as an example, Wang et al. (2023) found that at a total pressure of 10 MPa, the hydrogen fractional pressure increased from 1 MPa (a hydrogen blending ratio of 10%) to 1.5 MPa (a hydrogen blending ratio of 15%), which was associated with a significant increase in the sensitivity of the X80 steel to hydrogen embrittlement. Yuxin et al. (2022) found that the total pressure is 10 MPa, and that in general, X80 steel is not highly susceptible embrittlement, owing to plastic loss at hydrogen fractional pressures below 2 MPa (a hydrogen blending ratio of 20%). However, both these studies highlighted the fact that when the fractional pressure of hydrogen is higher than 1 MPa (a hydrogen blending ratio of 10%), the strength of the material is significantly reduced, which may pose hidden dangers to pipeline operation. In the present study, we calculated the fractional pressure of hydrogen at the upper wall of a natural gas pipeline using FLUENT software, and in Fig. 12, we present the estimated variations in hydrogen fractional pressure at different natural gas velocities using the three mixing methods.

As can be seen from Fig. 12, when T-type mixing is used, the fractional pressure of hydrogen declines with an increase in mixing distance. However, given that the density of hydrogen is less than that of natural gas, hydrogen tends to accumulate in the upper part of the pipeline, resulting in a high fractional pressure of hydrogen on the upper wall of the natural gas pipeline, thereby increasing the likelihood of hydrogen embrittlement. Contrastingly, when bending tube mixing is used, the fractional pressure of hydrogen increases with an increase in mixing distance, as under these conditions, hydrogen is incident from the middle of the pipeline. The closer the mixing point, the smaller is the volume fraction of hydrogen at the upper wall of the natural gas pipeline, as shown in Fig. 7. However, with an increase in mixing distance, hydrogen gradually diffuses to the upper wall of the natural gas pipeline, with a concomitant gradual increase in the fractional pressure of hydrogen on the upper wall. Conversely, when mixing using a static mixer, there is a rapid reduction in the fractional pressure of hydrogen with an increase in mixing distance, and on the basis of our simulation of working condition, we estimate that the fractional pressure of hydrogen at the pipeline outlet would reach 1.0 MPa.

3.2 Factors Influencing the Mixing Effect of Static Mixers

Our simulation-based analysis revealed that compared with T-tube and bending tube mixing, static mixers can be used to achieve 95% mixing uniformity over a shorter distance and with a higher mixing uniformity at the pipeline outlet, and thus has the overall best mixing effect. Accordingly, we subsequently examined the factors influencing the mixing by focusing on static mixers.

3.2.1 Velocity

The velocity of hydrogen can be calculated with reference to the velocity of natural gas and the hydrogen blending ratio (HBR). The ratio of the hydrogen inlet flow rate to the gas mixture flow rate is the hydrogen mixing ratio, which can be calculated by the following equation:

$$HBR = \frac{v_{H_2} d_{H_2}^2}{v_{CH_4} d_{CH_4}^2 + v_{H_2} d_{H_2}^2}, \tag{19}$$

where v_{H_2} is the velocity of hydrogen gas, d_{H_2} is the diameter of the hydrogen pipeline, v_{CH_4} is the velocity of natural gas, and d_{H_2} is the diameter of the natural gas pipeline.

The mixing of natural gas and hydrogen was simulated at natural gas velocities of 5, 10, and 15 m/s. Under the aforementioned conditions, the hydrogen blending ratio is 25%, and the velocities of hydrogen are 17.07, 34.13, and 51.2 m/s respectively. Figure 13 shows the variation in mixing uniformity σ with the distance from mixing point in response to different natural gas velocities.

As indicated in Fig. 13, increasing the velocity of natural gas has no significant effect on the blending uniformity of hydrogen and natural gas. By increasing the velocity of natural gas, the mixing uniformity of natural gas and hydrogen at the exit of the pipeline increased from 99.78% to 99.81%, and also contributed to an increase in the velocity of hydrogen, and more intense turbulence in the pipeline, thereby enhancing the mixing of natural gas and hydrogen. However, the increase of mixing uniformity is not obvious. With an increase in the velocity

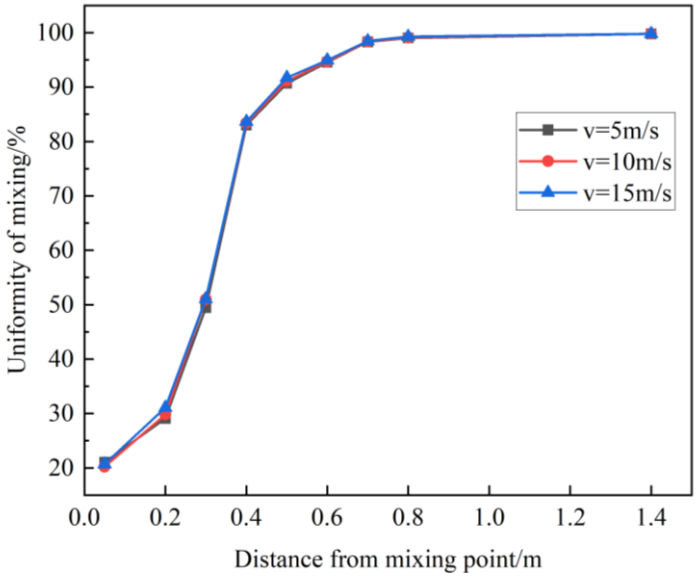

Fig. 13 Variations in mixing uniformity in response to different natural gas velocities

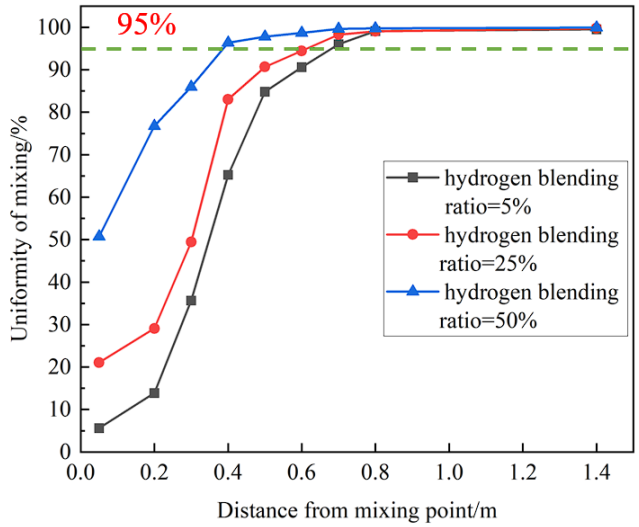

Fig. 14 Variations in mixing uniformity at different hydrogen blending ratios

of natural gas, the velocity of hydrogen in the pipeline reaches 51.2 m/s. In this regard, an excessive gas velocity will exacerbate corrosion and wear of the inner wall of the pipeline, which is not conducive to the operation and lifespan of gas pipelines.

3.2.2 Hydrogen Blending Ratio

In many countries and regions worldwide, the currently stipulated blending ratio for hydrogen and natural gas is 20%. Given the likely future developments in hydrogen blending technology, we simulated scenarios for the mixing of hydrogen and natural gas at hydrogen blending ratios of 5%, 25%, and 50% for a static mixer of 600 mm in length with a blade angle of 90°.

Figure 14 shows the variations in mixing uniformity σ with distance from the mixing point under different hydrogen blending ratios, from which it can be seen that increasing the hydrogen blending ratio can effectively improve the mixing uniformity of hydrogen and natural gas immediately after mixing. As the mixing distance increases, the mixing uniformities at the pipeline outlet at hydrogen blending ratio of 5%, 25%, and 50% increase to 99.49%, 99.78%, and 99.95%, respectively. Although this enhancement in mixing uniformity is not significant, increasing the hydrogen blending ratio would contribute to increasing the safety of gas for end users. Consequently, it is necessary to determine the range of hydrogen blending ratios based on actual situations.

3.2.3 Static Mixer Length

To study the effect of static mixer length on mixing uniformity, we calculated the mixing uniformity of natural gas and hydrogen at both the inlet and outlet of a static mixer. For the purpose of this analysis, we assessed the influence factor of static mixer on hydrogen volume fraction τ, which is defined as the ratio of mixing uniformity at the outlet of the static mixer to that at the inlet, as follows:

$$\tau = \frac{\sigma_{out}}{\sigma_{in}}, \tag{20}$$

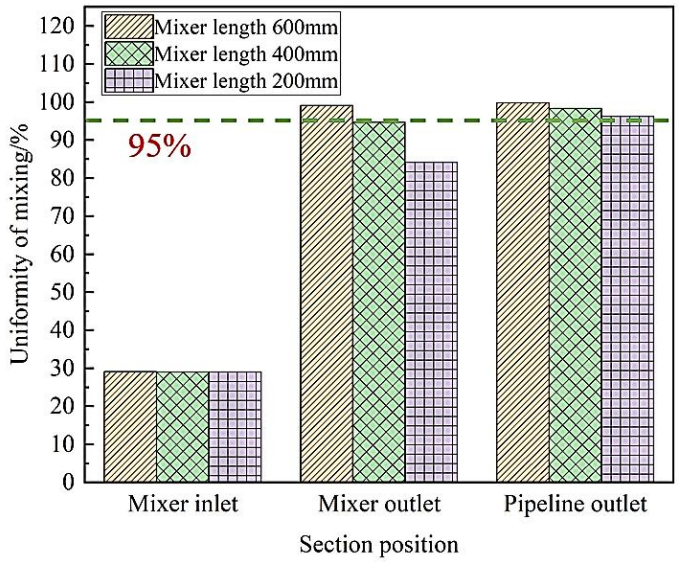

Fig. 15 Variations in mixing uniformity in different pipeline sections in static mixers of different lengths

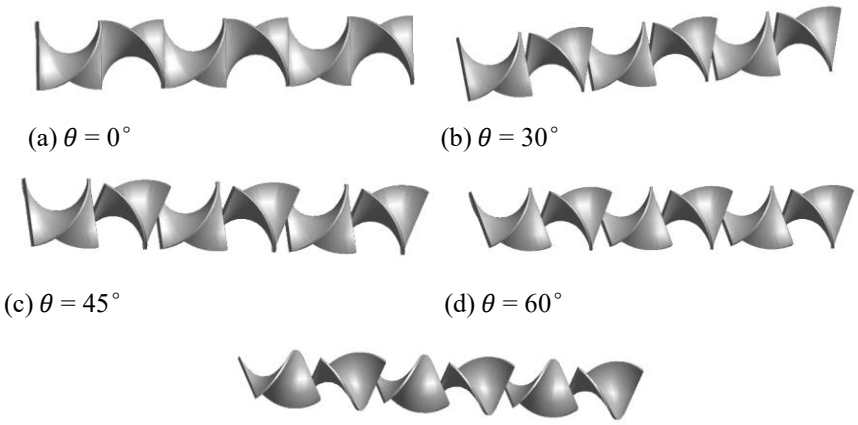

Fig. 16 Schematic diagrams of different-angled static mixer blades

where σ_{out} represents the uniformity of mixing at the outlet of the static mixer and σ_{in} represents the uniformity of mixing at the inlet of the static mixer. The larger the value of τ, the better is the mixing effect of the static mixer on natural gas and hydrogen.

The mixing of hydrogen and natural gas was simulated under conditions with static mixer lengths of 600, 400, and 200 mm at a hydrogen blending ratio of 25% and static mixer angle of 90°.

Figure 15 shows data regarding the mixing uniformity at the inlet and outlet of different-length static mixers, along with the mixing uniformity at the pipeline outlet, from which it can be seen that for static mixers of 200 and 400 mm in length, the mixing uniformities at the mixer outlet are 84.12% and 94.71%, respectively, which do not meet the industrial requirement of 95% mixing uniformity. Contratingly, for a static mixer of 600 mm in length, the mixing uniformity at the outlet is 99.05%, which accordingly meets industrial mixing requirements. At mixer lengths of 200, 400, and 600 mm, the corresponding influence factors on the hydrogen volume fraction τ are 2.90, 3.27, and 3.41, respectively, thereby indicating that the mixing effect of the static mixer increases with an increase in mixer length. This effect can be ascribed to increases in the velocities of the two gases in the static mixer, and a strong turbulence effect, and that the longer the length of the static mixer, the better is the mixing of the two gases.

3.2.4 Static Mixer Blade Angle

To examine the influence of the angle θ between static mixer blades on mixing uniformity, we simulated the mixing of hydrogen and natural gas for a static mixer of 600 mm with blade angles of 0°, 30°, 45°, 60°, or 90° at a hydrogen blending ratio of 25%. Figure 16 shows schematic representations of the blades of different angles, whereas Fig. 17 shows the variation in mixing uniformity with distance from the mixing point using different blade angles, and Fig. 18 shows the mixing uniformity at different positions in static mixers with different blade angles.

From Figs 17 and 18, it can be seen that at a blade angle of 0°, the mixing uniformities at the inlet and outlet

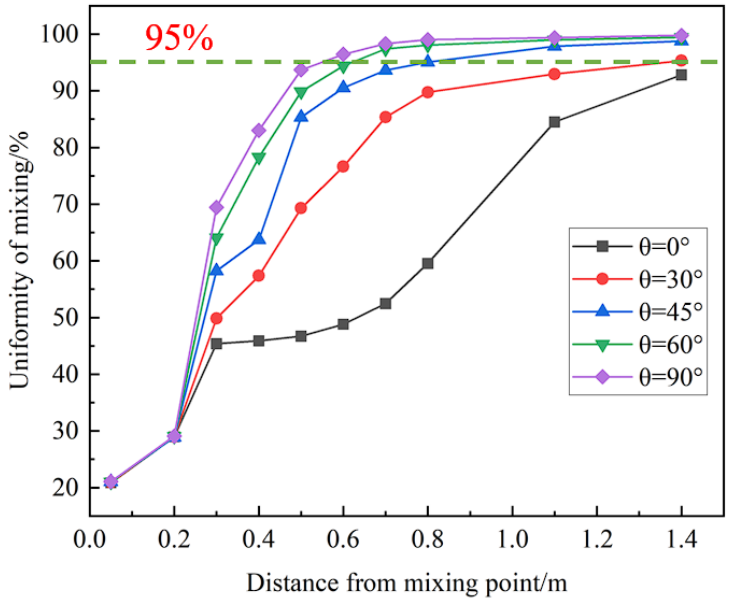

Fig. 17 Variations in mixing uniformity in static mixers with different blade angles

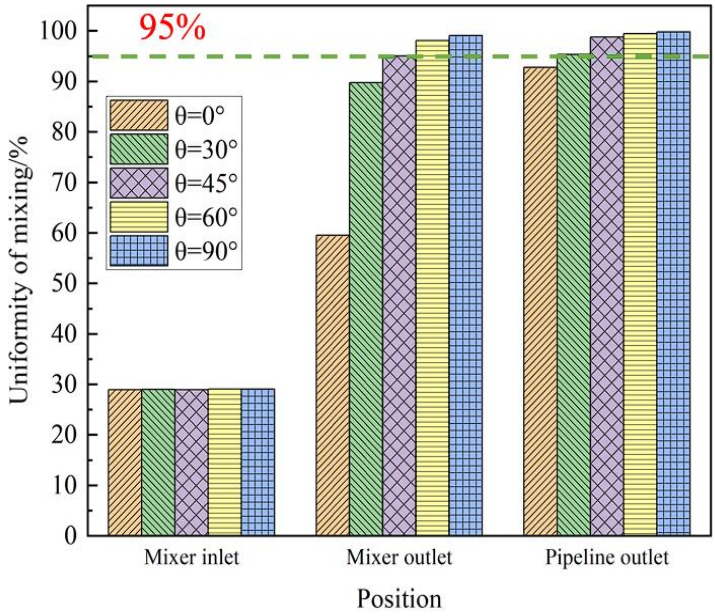

Fig. 18 Variations in mixing uniformity in different sections of a static mixer with different blade angles

of the static mixer are 28.96% and 59.53%, respectively, and influence factor of the static mixer on the volume fraction of hydrogen gas $\tau = 2.06$; at a blade angle of 30°, the mixing uniformities at the inlet and outlet are 28.99% and 89.75%, respectively, and $\tau = 3.10$; at a blade angle of 45°, the mixing uniformities at the inlet and outlet are 28.91% and 95.05%, respectively, and $\tau = 3.29$; at a blade angle of 60°, the mixing uniformities at the inlet and outlet are 29.03% and 99.46%, respectively, and $\tau = 3.426$; and at a blade angle of 90°, the mixing uniformities at the inlet and outlet are 29.08% and 99.78%, respectively, and $\tau = 3.431$. Accordingly, with an increase in the angle between the static mixer blades, there is an increase in the mixing effect of the static mixer.

4. CONCLUSION

In this study, we sought to determine the factors influencing the uniformity of mixing between hydrogen and natural gas using three different models, namely, T-tube, bending tube, and static mixer mixing, and used FLUENT software to perform numerical simulations based on these three mixing models. In these simulations we assessed the influence of hydrogen blending ratio and static mixer length and blade angle on the mixing of hydrogen and natural gas, on the basis of which, we draw the following conclusions.

(1) The uniformities of mixing at the outlet of the pipeline obtained using T-tube, bending tube, and static

mixer mixing are 96.13%, 99.40%, and 99.78% respectively, thereby indicating that the static mixer has the best effect regarding the mixing of hydrogen and natural gas. This effect can be attributed to the higher intensity of turbulence generated in the pipeline downstream of the mixing point when using a static mixer, which is conducive to the mixing of hydrogen and natural gas.

(2) Increasing the velocity of natural gas has no significant effect on the uniformity of hydrogen and natural gas blending, although an excessive rate of flow can adversely affect the service life of pipelines.

(3) Increasing the hydrogen blending ratio does not contribute to a significant enhancement of mixing uniformity at the pipeline outlet. Consequently, it is necessary to determine the hydrogen mixing ratio according to the technical conditions in practical engineering.

(4) For static mixers of lengths 200, 400, and 600 mm, we obtained mixing uniformity values of 84.12%, 94.71%, and 99.05% at the mixer outlet, respectively, with corresponding values of 2.97, 3.27, and 3.41 for the influence factor of static mixer on hydrogen volume fraction τ. These findings thus indicate that the mixing effect of the static mixer increases with an increase in mixer length.

(5) For static mixers with blade angles θ of 0°, 30°, 45°, 60°, and 90°, the mixing uniformity at the outlet of the mixer is 59.53%, 89.75%, 95.05%, 99.46%, and 99.78%, respectively, with corresponding values of 2.06, 3.10, 3.29, 3.426, and 3.431 for the influence factor of the static mixer on the volume fraction of hydrogen gas τ. These findings accordingly indicate that the mixing effect of static mixers increases with an increase in the angle between the mixer blades.

Given that an uneven mixing of hydrogen and natural gas can potentially lead to the damage of end-user gas equipment and reduces the calorific value of mixed gas, we believe that our findings in this study will provide theoretical guidance for the design of hydrogen mixing pipelines and the development of more efficient mixers, thereby contributing to the prevention of economic losses caused by the damage to gas equipment. This in turn would contribute to the more efficient utilization of hydrogen and natural gas and reduce the reliance on fossil fuels. Thus, these findings would have significant implications with respect to saving energy, reducing emissions, and the utilization of hydrogen energy. However, despite these promising features, certain technical problems remain to be resolved. For example, given the potential danger of performing mixing experiments for hydrogen and natural gas, we did not further verify the accuracy of the numerical simulation results under experimental conditions. In addition, owing to the constraints posed by numerical simulation modeling, we performed assessments considering only a horizontal pipeline, and did not take into account the potential influence of pipeline fluctuation on the hydrogen and natural gas mixing process in actual engineering. We nevertheless hope that future research will go some way to solving these and other unresolved issues.

CONFLICT OF INTEREST

The authors have no relevant financial or nonfinancial interests to disclose.

AUTHORS CONTRIBUTION

H. J. Zhao is mainly responsible for putting forward concepts, revising manuscripts, project management and obtaining funds, and can be a correspondent. **J. Du** is mainly responsible for research methods, data analysis and first draft writing, and can be the first author. **X. F. Lv** participated in research methods, data analysis and manuscript revision. Other authors (**S. W. Qiao**, **Z. H. Chen**) helped to organize the manuscript.

REFERENCES

Bing, Z., Xuexiu, Z., Bo, Z., & Suping, P. (2022). Industrial development of hydrogen blending in natural gas pipelines in china. *Strategic Study of Cae*, *24*(3), 100-107. http://doi.org/10.15302/J-SSCAE-2022.03.011

Cuiwei, L., Zhaoxue, C., Jiaxuan, Z., Yebin, P., Pengfei, D., Luling, L. I., Hongchao, Y., & Yuxing, L. I. (2022). Stratification in pipelines with hydrogen into natural gases. *Journal of China University of Petroleum (Edition of Natural Science)*, *46*(5), 153-161. http://doi.org/10.3969/j.issn.1673-5005.2022.05.017

Dadfarnia, M., Sofronis, P., Brouwer, J., & Sosa, S. (2019). Assessment of resistance to fatigue crack growth of natural gas line pipe steels carrying gas mixed with hydrogen. *International Journal of Hydrogen Energy*, *44*(21), 10808-10822. http://doi.org/10.1016/j.ijhydene.2019.02.216

Eames, I., Austin, M., & Wojcik, A. (2022). Injection of gaseous hydrogen into a natural gas pipeline. *International Journal of Hydrogen Energy*, *47*(61), 25745-25754. http://doi.org/10.1016/j.ijhydene.2022.05.300

Fang, L., Hongwei, Y., Yinshan, H., Yanjian, P., & Yuxia, Y. (2023). Effect of hydrogen-blending ratio of natural gas on performance of terminal gas equipment. *Low-Carbon Chemistry and Chemical Engineering*, *48*(2), 174-178. http://doi.org/10.3969/j.issn.1001-9219.2023.02.023

Hongjun, Z., Junwen, C., Huazhong, S. U., Tang, T., & Shan, H. E. (2022). Numerical investigation of the natural gas-hydrogen mixture stratification process in an undulating pipeline. *Journal of Southwest Petroleum University (Science & Technology Edition)*, *44*(6), 132-140. http://doi.org/10.11885/j.issn.1674-5086.2022.06.20.02

Hongjun, Z., Junwen, C., Tang, T., Xiaoyong, T., & Shan, H. E. (2023). Numerical simulation of the process of injecting hydrogen in natural gas pipeline. *Natural Gas and Oil*, *41*(2), 22-32. http://doi.org/10.3969/j.issn.1006-5539.2023.02.004

Liu, Q., Liu, Y., Li, S., Xu, H., Liang, G., Sun, C., & Sun, J. (2022). Analysis of the static mixer effect on natural gas mixing process in a pipeline. *Flow Measurement and Instrumentation*, *85*, 102146. http://doi.org/10.1016/j.flowmeasinst.2022.102146

Liu, Y., Rao, A., Ma, F., Li, X., Wang, J., & Xiao, Q. (2023). Investigation on mixing characteristics of hydrogen and natural gas fuel based on SMX static mixer. *Chemical Engineering Research and Design*, *197*, 738-749. http://doi.org/10.1016/j.cherd.2023.07.040

Mingxing, S. (2012). *The CFD Numerical Simulation of Rapid Gas-gas Mixing* [Master Thesis, East China University of Science and Technology], Shanghai.

Mazloomi, K., & Gomes, C. (2012). Hydrogen as an energy carrier: Prospects and challenges. *Renewable and Sustainable Energy Reviews*, *16*(5), 3024-3033. http://doi.org/10.1016/j.rser.2012.02.028

SHhangze, L., Qing, Y., & Jian, G. (2022). Current situation and prospects of hydrogen energy utilization and industrial development. *Energy and Energy Conservation*, (11), 18-21. http://doi.org/10.16643/j.cnki.14-1360/td.2022.11.038.

Shijie, S., Xiaopeng, L., & Shan, L. (2019). Research on technology of blending hydrogen into natural gas. *Yunnan Chemical Technology*, *46*(6), 70-72. http://doi.org/10.3969/j.issn.1004-275X.2019.06.027

Wang, C., Zhang, J., Liu, C., Hu, Q., Zhang, R., Xu, X., Yang, H., Ning, Y., & Li, Y. (2023). Study on hydrogen embrittlement susceptibility of X80 steel through in-situ gaseous hydrogen permeation and slow strain rate tensile tests. *International Journal of Hydrogen Energy*, *48*(1), 243-256. http://doi.org/10.1016/j.ijhydene.2022.09.228

Wei, H., Duan, B., Shi, X., Gao, R., Hua, Z., Qiu, S., & Zhao, Y. (2023). Influence of hydrogen in natural gas mixed hydrogen environment on mechanical properties of X80 pipeline steel. *International Journal of Hydrogen Energy*. http://doi.org/10.1016/j.ijhydene.2023.09.138

Yongwei, A., Chen, S., Shouhu, J., Guanwei, J., Weiqing, X., Wei, L., Liang, Z., & Maolin, C. (2022). Hydrogen concentration distribution in flow of hydrogen blended to natural gas in pipeline. *Mechanics in Engineering*, *44*(04), 767-775. http://doi.org/10.6052/1000-0879-22-381

Yue, S. U., Jingfa, L. I., Bo, Y. U., Yanlin, Z., Jianli, L. I., & Dongxu, H. (2023). Simulation study on the mixing of hydrogen and natural gas in static mixers. *Natural Gas Industry*, *43*(3), 113-122. http://doi.org/10.3787/j.issn.1000-0976.2023.03.012

Yuxin, L. I., Rui, Z., Cuiwei, L., Cailin, W., Hongchao, Y., Qihui, H. U., Jiaxuan, Z., Xiusai, X. U., & Huimin, Z. (2022). Hydrogen embrittlement behavior of typical hydrogen-blended natural gas pipeline steel. *Oil & Gas Storage and Transportation*, *41*(6), 732-742. http://doi.org/10.6047/j.issn.1000-8241.2022.06.015

Yuxuan, L. (2022). An overview of hydrogen energy and its applications. *Energy Conservation*, *41*(10), 78-80. http://doi.org/10.3969/j.issn.1004-7948.2022.10.022

Zhen, H., Chuang, L., Yanbing, Z., Xianming, Y., & Xiaodong, C. (2021). Feasibility analysis of natural gas mixed with hydrogen in my country. *Yunnan Chemical Technology*, *48*(10), 94-96. http://doi.org/10.3969/j.issn.1004-275X.2021.10.28